


 Cite this: *RSC Adv.*, 2021, **11**, 24022

Received 3rd April 2021
 Accepted 26th June 2021
 DOI: 10.1039/d1ra02627e
rsc.li/rsc-advances

Introduction

Stimuli-responsive fluorescent molecules are of interest for their analytical applications in environmental chemistry and life sciences.¹ Acid-/base-induced fluorescence is especially useful when monitoring living systems, because it allows non-invasive, real-time imaging with high spatiotemporal resolution of biological processes that occur with changes in pH.² Simple one-step (off-on or on-off) fluorescence switching processes, mediated by acids and bases, have been investigated widely in living systems, using fluorescein,³ BODIPY,⁴ rhodamine,⁵ naphthalimide,⁶ pyrene,⁷ hemicyanine,⁸ quinoline⁹ and benzimidazole derivatives¹⁰ as fluorophores.

Although many systems have been reported displaying simple one-step fluorescence switching, developing more complicated two- or more-step fluorescence processes—such as “off-on-off” or “on-off-on” systems—has remained challenging.¹¹ Clear examples of two- and three-step fluorescence switching, mediated by acids and bases, have been limited to specific cases using, for example, 9-anthrylmethyl-bis(2-picoly) amine,¹² dimethylamino-substituted BF_3 azadipyrromethenes,¹³ a catechol derivative,¹⁴ benzoxazole-substituted 7-hydroxy-ycoumarin,¹⁵ and borylated arylisoquinolines.¹¹ These multi-state fluorophores have the potential to be applied as more functionalized pH probes providing responses beyond the binary.

In this paper we present the fluorescence changes that occur upon the base-induced three-step deprotonation of a trefoil-shaped salicylaldehyde azine (SA) derivative (**1**) bearing multiple acidic protons. SA units have been investigated previously as typical fluorophores displaying aggregation-induced

emission (AIE).¹⁶ Because of the acidity of the phenolic OH groups in the SA skeleton, one-step deprotonation and fluorescence change mediated by base have been reported for simple symmetric SA derivatives.^{16b,c,17} Based on the deprotonation ability and fluorescence of the SA substructure, we synthesized the more complicated unsymmetrical trefoil-shaped SA derivative **1** with the anticipation that it might display multi-state fluorescence upon varying the concentration of base (Fig. 1). The azine **1** possesses six acidic protons (in consideration of tautomer of phenolic form): three in the [6] radialene-type central unit and three on the SA-type outer “leaves.” This planar molecule possesses a single π -conjugated system, which facilitates base-induced stepwise deprotonation.

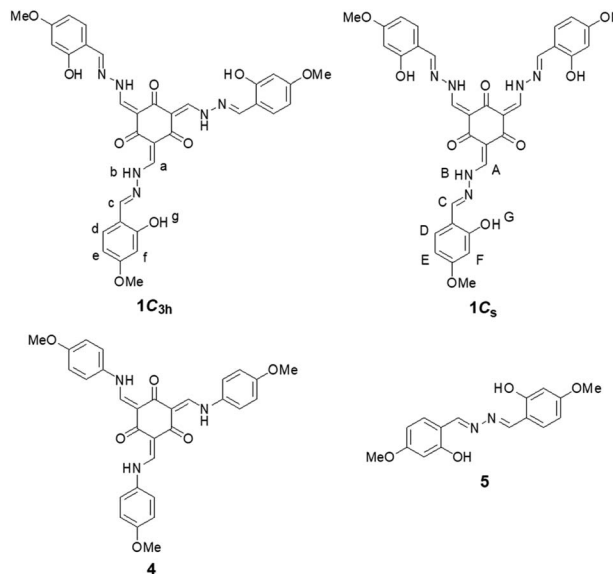


Fig. 1 Structures of the trefoil-shaped azine **1C_{3h}**, its geometric isomer **1C_s**, and analogues of their central unit (**4**) and outer “leaves” (**5**). Annotations with capital letters: **1C_s**; lower-case letters: **1C_{3h}**.

Department of Materials Science and Engineering, Faculty of Engineering, University of Fukui, Bunkyo, Fukui 910-8507, Japan. E-mail: naito-m@u-fukui.ac.jp; tokunaga@u-fukui.ac.jp

† Electronic supplementary information (ESI) available. See DOI: 10.1039/d1ra02627e



Results and discussion

Synthesis and structure of the trefoil-shaped azine **1**

We synthesized the trefoil-shaped azine **1** in a yield of 48% after mixing 4-methoxysalicylaldehyde hydrazone (**2**) and 1,3,5-triformylphloroglucinol (**3**) in CHCl_3 (Scheme 1). We also prepared tris(*N*-4-methoxysalicylideneaniline) (**4**)¹⁸ and 4-methoxysalicylaldehyde azine (**5**)^{16b} as structural analogues of the central unit and outer leaf of **1**, respectively (Fig. 1). ^1H NMR spectroscopic analysis of **1** in $\text{DMSO}-d_6$ at room temperature revealed that the keto tautomer was the predominant form, present as an equilibrium mixture of the two geometric isomers **1C_{3h}** and **1C_s** having C_{3h} and C_s symmetries, respectively. Through integration of the signals of the both of these species, we calculated the ratio of **1C_{3h}** to **1C_s** in this solution to be 1 : 2. The spectrum featured a complicated peak pattern that originated from the four different types of SA “leaves” of the two isomeric structures: one set from the three equivalent leaves in **1C_{3h}** and the other three from the three non-equivalent leaves of **1C_s** (Fig. 2 and S8†). Similar complexity was reported previously by MacLachlan for equilibrium mixtures of the two geometric isomers of **4** having C_{3h} and C_s symmetries.¹⁸ Variable-temperature (293–393 K) ^1H NMR spectroscopic analysis of **1** in $\text{DMSO}-d_6$ revealed that the initially split signals of the imino (H_a/H_A , H_c/H_C), NH (H_b/H_B), aromatic (H_d/H_D), and OH (H_g/H_G) units coalesced upon elevating the temperature to 373 K (Fig. S1†). These spectra confirmed that **1** was present as an equilibrium mixture of the two geometric isomers **1C_{3h}** and **1C_s** in $\text{DMSO}-d_6$ and that their rate of equilibration was slow on the NMR spectroscopic timescale at room temperature.

^1H NMR spectroscopic titration of **1** with base

We used ^1H NMR spectroscopy to investigate the deprotonation processes of **1** upon successive addition of base in $\text{DMSO}-d_6$. In the ^1H NMR titration spectra of **1** (5.0 mM in $\text{DMSO}-d_6$) with 0–1

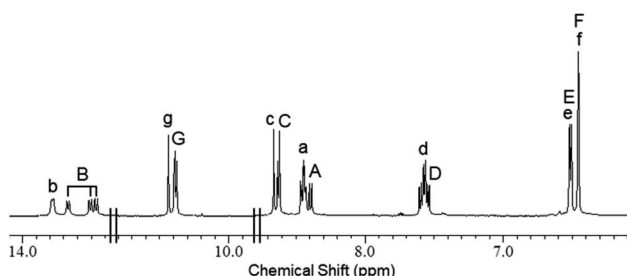
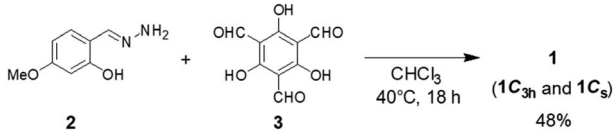


Fig. 2 ^1H NMR spectrum of **1** ($\text{DMSO}-d_6$, 600 MHz, 298 K). Annotations with capital letters: **1C_s**; lower-case letters: **1C_{3h}**.

eq. of aq. NaOH (300 mM), the four doublets corresponding to the imino protons H_a and H_A of the central unit at 8.39–8.47 ppm became fused into a broad and downfield-shifted peak at 8.75 ppm after the addition of 1 eq. of base (Fig. 3 and S2†). The broadening indicated that deprotonation accelerated the equilibration between the C_{3h} and C_s isomers. Similar broadening of the signals of the imino protons was observed for **4**, a structural analogue of the central unit of **1**; in this case, the signals of the imino protons of **4** at 8.52–8.60 ppm were fused with broadening and shifted slightly upfield to 8.50 ppm upon increasing the amount of base from 0 to 1 eq. (Fig. S3†). These observations suggested that one of the NH protons (H_b/H_B) of the central unit of **1** was deprotonated in the first step after the addition of 1 eq. of base. In the titration experiments of **1** with 1–4 eq. of base, the signals of the aromatic protons of the outer leaves (H_e/H_E and H_f/H_F at 6.52 and 6.48 ppm, respectively) were broadened until 3 eq. of base had been added, with new peaks appearing in the upfield region after the addition of 4 eq. of base; these new signals sharpened at 5.71 (H_e/H_E) and 5.85 (H_f/H_F) ppm in the presence of 12 eq. of base (Fig. 3 and S2†). Similar broadening and upfield-shifting of the signals for the aromatic protons were observed in the spectrum of **5**, a structural analogue of the outer leaves of **1**; indeed, the signals of the aromatic protons of **5** at 6.56 and 6.51 ppm broadened and shifted upfield to 5.61 and 5.77 ppm, respectively, upon increasing the amount of base from 0 to 3 eq. (Fig. S4†). These findings suggest that some of the OH protons H_g/H_G of the outer leaves of **1** were deprotonated in a subsequent step when greater than 1 eq. of base was added. The base-induced spectral changes were restored to the original state upon neutralization using trifluoroacetic acid (TFA), indicating that these deprotonation/protonation processes were reversible and maintained the trefoil-shaped structure (Fig. S5†). The restored spectra were, however, observed with small amounts of

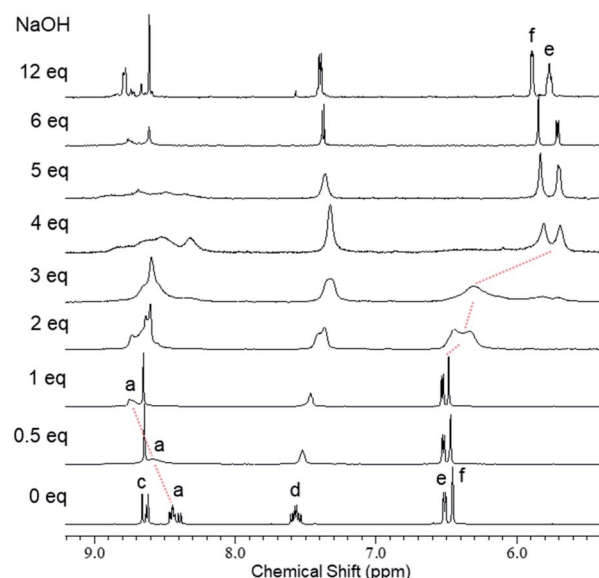


Fig. 3 ^1H NMR spectra (600 MHz, $\text{DMSO}-d_6$, 295 K) of **1** (5.0 mM) recorded after successive addition of NaOH (0–12 eq.).



new signals, presumably because the acid induced partial decomposition of the azine. We conclude that **1** was deprotonated in a stepwise manner upon adding base, with one of the NH moieties of the central unit deprotonated in the first step and then successive addition of base inducing the deprotonation of some of the OH groups of the outer leaves.¹⁹

UV-vis absorption spectra of **1** with base

UV-vis absorption spectra of **1** in the presence of base supported the stepwise deprotonation observed in the ¹H NMR spectra. In the UV-vis absorption spectra of **1** [1.0×10^{-1} mM in DMSO/H₂O = 20 : 1 (v/v)] recorded with 0–1 eq. of NaOH, the absorption band near 425 nm decreased in intensity with isosbestic points at 387 and 457 nm after adding the base (Fig. 4a). We observed a similar behavior for an absorption band of **4**, where the signal near 411 nm decreased in intensity with isosbestic points at 400 and 456 nm upon the addition of up to 3 eq. of base (Fig. S6†). These observations suggested that one of the NH moieties of the central unit of **1** was deprotonated in the first step upon the addition of 1 eq. of base, consistent with the ¹H NMR spectral data. After increasing the amount of base from 1 to 6 eq., the UV-vis absorption spectra of **1** revealed that the absorption band near 470 nm increased in intensity with an isosbestic point at 440 nm (Fig. 4b). Similar behavior occurred for **5**; its absorption band near 447 nm increased in intensity with an isosbestic point at 400 nm upon the addition of up to 3 eq. of base (Fig. S7†). These observations suggested that one of the OH groups of the outer leaves of **1** was deprotonated in the second step when greater than 1 eq. of base had been added, consistent with the results of the ¹H NMR spectroscopic experiments.

We recorded additional UV-vis absorption spectra to investigate the deprotonation of **1** in the presence of excessive amounts of base. In the UV-vis absorption spectra of **1** with 6–20 eq. of base, the absorption band blue-shifted from 470 to 425 nm upon increasing the amount of base (Fig. 4c). This peak shift seemed to be not accompanied by any isosbestic points, indicating that this step involved competitive deprotonation of the NH moieties of the central unit and of the OH groups of the

outer leaves of **1**. Fig. S6† reveals that **4** underwent deprotonation of one of its NH moieties in the first step after the addition of 3 eq. of base, with subsequent addition of 14 eq. of base resulting in deprotonation of a second NH moiety (characterized by the increasing intensity of the absorption band near 391 nm with isosbestic points at 355 and 400 nm). These observations suggest that two of the NH moieties of the central unit of **1** can be deprotonated upon the addition of excessive amounts of base. Fig. S7† indicates that one of the OH groups of **5** was deprotonated after the addition of 3 eq. of base; subsequent addition of 10 eq. of base led to deprotonation of the other OH group, as revealed by the increasing intensity of the absorption band near 437 nm with an isosbestic point at 358 nm. Thus, all of the OH protons of the outer leaves of **1** could be deprotonated after the addition of an excessive amount of base. In particular, our results suggest that **1** formed a pentaanion after the addition of excessive base, with deprotonation of two of the NH moieties of the central unit and the three OH groups of the outer leaves.

Base-induced multi-state fluorescence of **1**

The trefoil-shaped azine **1** exhibited multi-state fluorescence in solution upon successive addition of base. The emission properties of **1** [1.0×10^{-1} mM in DMSO/H₂O = 20 : 1 (v/v)] under UV irradiation ($\lambda_{\text{ex}} = 365$ nm) changed in three steps (Fig. 5) upon the gradual addition of up to 20 eq. of NaOH: initially yellow (0 eq. of base) and then changing to weak yellow (1 eq.), to strong yellow (6 eq.), and, finally, to a cyan emission (20 eq.).

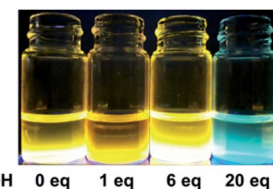


Fig. 5 Photograph of solutions of **1** (1.0×10^{-1} mM) in the presence of 0–20 eq. of NaOH under UV irradiation [DMSO/H₂O = 20 : 1 (v/v); $\lambda_{\text{ex}} = 365$ nm].

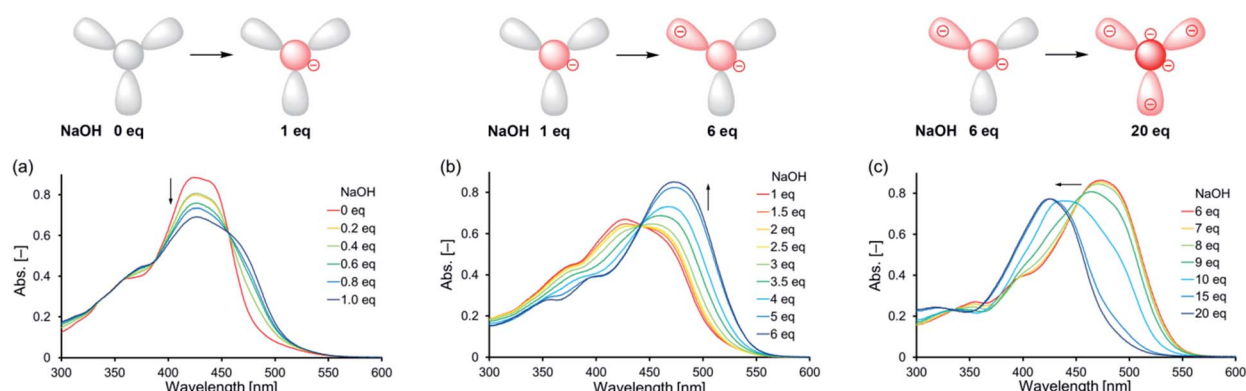


Fig. 4 Schematic representations of the proposed deprotonation steps and UV-vis absorption spectra of **1** (1.0×10^{-1} mM) in the presence of (a) 0–1.0, (b) 1–6, and (c) 6–20 eq. of NaOH [DMSO/H₂O = 20 : 1 (v/v); $d = 1$ mm].



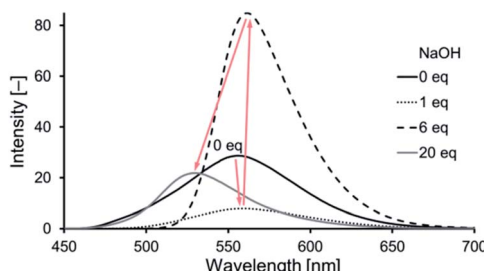


Fig. 6 Emission spectra of **1** (black solid line) in the presence of 1 (dotted line), 6 (dashed line), and 20 (gray solid line) eq. of NaOH [DMSO/H₂O = 20 : 1 (v/v); 1.0 × 10⁻¹ mM; $\lambda_{\text{ex}} = 440$ nm].

This three-step change in the emission of **1**, induced by base in solution, was revealed in its emission spectra (Fig. 6). Comparing the emission spectra ($\lambda_{\text{ex}} = 440$ nm) of **1** in the absence and presence (1 eq.) of base in solution, the peak of the signal was slightly red-shifted from 552 to 560 nm, whereas its intensity decreased to approximately one-third of the initial value, after the addition of base (Fig. 6, from black solid to dotted line). Upon increasing the amount of base from 1 to 6 eq., the peak of the signal was slightly red-shifted to 562 nm and the intensity increased significantly by approximately 10 times (Fig. 6, from black dotted to dashed line). The emission spectrum recorded in the presence of 20 eq. of base revealed a considerable blue-shift of the peak of the signal from 562 to 530 nm, with a decrease in intensity to approximately a quarter of the previous value (Fig. 6, from black dashed to gray line). The ¹H NMR and UV-vis absorption spectra suggested that **1** formed a monoanion after the addition of 1 eq. of base, through deprotonation of one of the NH moieties of the central unit; it then formed a dianion after the addition of 6 eq. of base, through subsequent deprotonation of one of the OH groups of the outer leaves; finally, it formed a pentaanion after the addition of 20 eq. of base, through deprotonation of two of the NH moieties of the central unit and all three of the OH groups of the outer leaves. On the basis of the assumption that the deprotonation relate to the fluorescence, we propose that these deprotonation steps of **1** were accompanied by a three-step change in its emission properties upon varying the content of base in the solution: a decrease in intensity after forming the monoanion through the first-step deprotonation; an increase in intensity after forming the dianion through the second-step deprotonation; and a change in color after forming the pentaanion through the third-step deprotonation.

Conclusions

We have demonstrated the base-induced three-step changes in fluorescence of a trefoil-shaped azine bearing multiple acidic protons. This azine was readily synthesized from 1,3,5-triformylphloroglucinol and 4-methoxysalicylaldehyde hydrazone. ¹H NMR spectroscopic analysis confirmed the tautomerization of the azine in solution. ¹H NMR and UV-vis absorption and emission spectroscopy revealed the three-step process of the deprotonation of the azine upon the addition of base. Further

research is currently underway to obtain acid-/base-induced fluorescence switch of the azine.

Experimental

Materials and general methods

4-Methoxysalicylaldehyde hydrazone (**2**)²⁰ 1,3,5-triformylphloroglucinol (**3**)¹⁸ tris(N-4-methoxysalicylideneaniline) (**4**)¹⁸ and 4-methoxysalicylaldehyde azine (**5**)^{16b} were prepared according to procedures reported previously. All solvents and chemicals were obtained from commercial sources and used without further purification. ¹H and ¹³C NMR spectra were recorded using JEOL ECA-600II spectrometer with DMSO-*d*₅ (2.49 ppm for ¹H NMR) and DMSO-*d*₆ (39.5 ppm for ¹³C NMR) as internal references. Mass spectra were recorded using a JEOL JMS-700T spectrometer. Infrared (IR) spectra were recorded using a JASCO FT/IR-4100 spectrometer. UV-vis absorption spectra were recorded using a HITACHI U-3900H spectrometer. Fluorescence spectra were recorded using a JASCO FP-8500 spectrophotometer.

Synthesis of the trefoil-shaped azine (1**).** A solution of 4-methoxysalicylaldehyde hydrazone (**2**, 0.500 g, 3.01 mmol) and 1,3,5-triformylphloroglucinol (**3**, 0.211 g, 1.00 mmol) in CHCl₃ (30 mL) was stirred at 40 °C for 18 h. After evaporation of the solvent, the residue was washed by Et₂O (150 mL) to give **1** (0.317 g, 48%) as an orange powder. Mp 230 °C (decomp.). IR (KBr, ν_{max}): 3436, 3004, 2937, 2840, 1607, 1510, 1457, 1372, 1283, 1233, 1166, 1138, 1118, 1030, 964, 836, 668 cm⁻¹. ¹H NMR (600 MHz, DMSO-*d*₆): δ 13.78 (d, *J* = 8.9 Hz, minor 3H, H_b), 13.67 (d, *J* = 10.7 Hz, major 1H, H_B), 13.51 (d, *J* = 11.2 Hz, major 1H, H_B), 13.47 (d, *J* = 11.2 Hz, major 1H, H_B), 10.44 (s, minor 3H, H_g), 10.40 (s, major 1H, H_G), 10.39 (s, major 1H, H_G), 10.38 (s, major 1H, H_G), 8.66 (s, minor 3H, H_c), 8.63 (s, major 1H, H_C), 8.62 (s, major 2H, H_C), 8.46 (d, *J* = 11.2 Hz, major 1H, H_A), 8.45 (d, *J* = 10.7 Hz, major 1H, H_A), 8.44 (d, *J* = 8.9 Hz, minor 3H, H_a), 8.40 (d, *J* = 11.2 Hz, major 1H, H_A), 7.60 (d, *J* = 8.7 Hz, major 1H, H_D), 7.58 (d, *J* = 8.7 Hz, major 1H, H_D), 7.57 (d, *J* = 8.7 Hz, minor 3H, H_d), 7.54 (d, *J* = 8.7 Hz, major 1H, H_D), 6.51 (dd, *J* = 8.7, 1.8 Hz, each major 3H and minor 3H, H_E and H_e), 6.46 (d, *J* = 1.8 Hz, each major 3H and minor 3H, H_F and H_f), 3.76 [(s, major 6H, OCH₃) and (s, minor 9H, OCH₃)], 3.75 (s, major 3H, OCH₃) ppm. ¹³C NMR (150 MHz, DMSO-*d*₆): δ 185.7, 182.9, 182.2, 180.4, 162.95, 162.87, 159.1, 159.0, 158.9, 151.7, 151.3, 151.1, 151.0, 150.6, 150.2, 149.9, 149.6, 129.6, 129.4, 129.1, 128.9, 111.9, 106.9, 104.1, 103.9, 103.8, 103.5, 101.0, 55.3 ppm. HRMS (FAB) *m/z* calcd for C₃₃H₃₁N₆O₉⁺ [M + H]⁺ 655.2153, found 655.2142.

Author contributions

N. T. performed the experiments. M. N. wrote the manuscript. S. M. performed the analysis. Y. T. edited the manuscript. M. N. and Y. T. directed the project.

Conflicts of interest

There are no conflicts to declare.

Acknowledgements

This study was supported by the Research Center for Fibers and Materials at the University of Fukui.

Notes and references

1 (a) A. P. de Silva, H. Q. N. Gunaratne, T. Gunnlaugsson, A. J. M. Huxley, C. P. McCoy, J. T. Rademacher and T. E. Rice, Signaling recognition events with fluorescent sensors and switches, *Chem. Rev.*, 1997, **97**, 1515–1566; (b) R. Martínez-Máñez and F. Sancenón, Fluorogenic and chromogenic chemosensors and reagents for anions, *Chem. Rev.*, 2003, **103**, 4419–4476.

2 (a) J.-T. Hou, W. X. Ren, K. Li, J. Seo, A. Sharma, X.-Q. Yu and J. S. Kim, Fluorescent bioimaging of pH: from design to applications, *Chem. Soc. Rev.*, 2017, **46**, 2076–2090; (b) A. Méndez-Ardoy, J. J. Reina and J. Montenegro, Synthesis and supramolecular functional assemblies of ratiometric pH probes, *Chem. -Eur. J.*, 2020, **26**, 7516–7536.

3 C. He, K. Lu and W. Lin, Nanoscale metal-organic frameworks for real-time intracellular pH sensing in live cells, *J. Am. Chem. Soc.*, 2014, **136**, 12253–12256.

4 (a) N. Boens, V. Leen and W. Dehaen, Fluorescent indicators based on BODIPY, *Chem. Soc. Rev.*, 2012, **41**, 1130–1172; (b) M. Grossi, M. Morgunova, S. Cheung, D. Scholz, E. Conroy, M. Terrile, A. Panarella, J. C. Simpson, W. M. Gallagher and D. F. O'Shea, Lysosome triggered near-infrared fluorescence imaging of cellular trafficking processes in real time, *Nat. Commun.*, 2016, **7**, 10855.

5 H. Zhu, J. Fan, Q. Xu, H. Li, J. Wang, P. Gao and X. Peng, Imaging of lysosomal pH changes with a fluorescent sensor containing a novel lysosome-locating group, *Chem. Commun.*, 2012, **48**, 11766–11768.

6 M. H. Lee, N. Park, C. Yi, J. H. Han, J. H. Hong, K. P. Kim, D. H. Kang, J. L. Sessler, C. Kang and J. S. Kim, Mitochondria-immobilized pH-sensitive off-on fluorescent probe, *J. Am. Chem. Soc.*, 2014, **136**, 14136–14142.

7 L. Cao, Z. Zhao, T. Zhang, X. Guo, S. Wang, S. Li, Y. Li and G. Yang, *In vivo* observation of the pH alternation in mitochondria for various external stimuli, *Chem. Commun.*, 2015, **51**, 17324–17327.

8 Q. Wan, S. Chen, W. Shi, L. Li and H. Ma, Lysosomal pH rise during heat shock monitored by a lysosome-targeting near-infrared ratiometric fluorescent probe, *Angew. Chem., Int. Ed.*, 2014, **53**, 10916–10920.

9 G. Li, D. Zhu, L. Xue and H. Jiang, Quinoline-based fluorescent probe for ratiometric detection of lysosomal pH, *Org. Lett.*, 2013, **15**, 5020–5023.

10 H. J. Kim, C. H. Heo and H. M. Kim, Benzimidazole-based ratiometric two-photon fluorescent probes for acidic pH in live cells and tissues, *J. Am. Chem. Soc.*, 2013, **135**, 17969–17977.

11 V. F. Pais, M. Lineros, R. López-Rodríguez, H. S. El-Sheshtawy, R. Fernández, J. M. Lassaletta, A. Ros and U. Pischel, Preparation and pH-switching of fluorescent borylated arylisoquinolines for multilevel molecular logic, *J. Org. Chem.*, 2013, **78**, 7949–7961.

12 S. A. de Silva, A. Zavaleta, D. E. Baron, O. Allam, E. V. Isidor, N. Kashimura and J. M. Percario, A fluorescent photoinduced electron transfer sensor for cations with an off-on-off proton switch, *Tetrahedron Lett.*, 1997, **38**, 2237–2240.

13 S. O. McDonnell and D. F. O'Shea, Near-infrared sensing properties of dimethylamino-substituted BF_2 -azadipyrromethenes, *Org. Lett.*, 2006, **8**, 3493–3496.

14 E. Evangelio, J. Hernando, I. Imaz, G. G. Bardají, R. Alibés, F. Busqué and D. Ruiz-Molina, Catechol derivatives as fluorescent chemosensors for wide-range pH detection, *Chem. -Eur. J.*, 2008, **14**, 9754–9763.

15 K. K. Sadhu, S. Mizukami, A. Yoshimura and K. Kikuchi, pH Induced dual “OFF-ON-OFF” switch: influence of a suitably placed carboxylic acid, *Org. Biomol. Chem.*, 2013, **11**, 563–568.

16 (a) W. Tang, Y. Xiang and A. Tong, Salicylaldehyde azines as fluorophores of aggregation-induced emission enhancement characteristics, *J. Org. Chem.*, 2009, **74**, 2163–2166; (b) X. Ma, J. Cheng, J. Liu, X. Zhou and H. Xiang, Ratiometric fluorescent pH probes based on aggregation-induced emission-active salicylaldehyde azines, *New J. Chem.*, 2015, **39**, 492–500; (c) J. Yang, J. Rui, X. Xu, Y. Yang, J. Su, H. Xu, Y. Wang, N. Sun and S. Wang, Fluorescence staining of salicylaldehyde azine, and applications in the determination of potassium *tert*-butoxide, *RSC Adv.*, 2016, **6**, 30636–30641.

17 M. Ziółek, M. Gil, J. A. Organero and A. Douhal, What is the difference between the dynamics of anion- and keto-type of photochromic salicylaldehyde azine?, *Phys. Chem. Chem. Phys.*, 2010, **12**, 2107–2115.

18 J. H. Chong, M. Sauer, B. O. Patrick and M. J. MacLachlan, Highly stable keto-enamine salicylideneanilines, *Org. Lett.*, 2003, **5**, 3823–3826.

19 We also tried using triethylamine as base, however, the deprotonation was stopped at first step even in the presence of excessive amounts of the base (Fig. S9†).

20 F. M. F. Santos, J. N. Rosa, N. R. Candeias, C. P. Carvalho, A. I. Matos, A. E. Ventura, H. F. Florindo, L. C. Silva, U. Pischel and P. M. P. Gois, A three-component assembly promoted by boronic acids delivers a modular fluorophore platform (BASHY dyes), *Chem. -Eur. J.*, 2016, **22**, 1631–1637.

